A Review of Ground-Based Remote Sensing of Temperature and Moisture by Passive Microwave Radiometers

JAN I. H. ASKNE, MEMBER, IEEE, AND ED R. WESTWATER

Abstract—**Remote sounding of atmospheric variables by ground-based microwave radiometers has proved to be useful for several applications. These radiometers are used to measure profiles or integrated values of temperature, water vapor, and cloud liquid. The information provided is useful in meteorology, astronomy, geodesy, communication, for correction of space observations, for atmospheric research, etc. It may be possible to combine ground-based radiometers, satellite-borne radiometers, and VHF radars to form a meteorological network which provides profiles of temperature, humidity, and wind continuously in time. This paper will review some of the developments in this area, describe basic principles and results of field experiments, including the recent ONSAM-experiment, and summarize two years' performance of the NOAA Profiler.**

I. Introduction

OBSERVATIONS of atmospheric variables such as temperature and water vapor are important in many applications such as meteorology, communications, and astronomy. Existing meteorological observational systems use radiosondes (RAOB's) launched every 12 h at stations spaced roughly 350 km apart over important parts of the land area. This system does not provide adequate information for many applications even in meteorology. Nowcasting is such an example, e.g., forecasts for a period 0–12 h ahead. On that time scale we have many important short-lived phenomenon of interest including front movements, build up of convective clouds, etc. This situation can be improved by remote sensing, including ground-based microwave radiometers, satellite-borne downward-looking radiometer systems, wind-sensing radars, etc.

The interest in ground-based microwave radiometry goes back to the possibility to build an "all weather" system which can be operated more or less continuously and automatically. This equipment may be used as a complement to RAOB's. However, there is as well an interest to replace the expensive radiosonde service. Although the vertical resolution of radiometrically derived temperature and humidity profiles is much coarser than that of RAOB's integrated quantities such as pressure heights, pressure thicknesses, and precipitable water vapor are determined with an accuracy comparable to RAOB's [1], [2]. In addition, some quantities derived from radiometers are not easily measurable by other means. These would include liquid water content of clouds and integrated water vapor in some arbitrary direction.

Ground-based microwave radiometry for atmospheric sounding purposes has been developed over many years at the Wave Propagation Laboratory of the NOAA/ERL in Boulder, Colorado, where an automatic profiler for wind, temperature, and humidity is now in use [2]. Other similarly directed microwave radiometers are described in the literature [3]–[7].

The work at the Chalmers University of Technology (CUT) was initiated through the desire to monitor atmospheric humidity in connection with radio-astronomical measurements. Tests of the water-vapor radiometer for meteorological applications were made in 1980 [7], [8]. Somewhat later, a new design of a radiometer for temperature profiling was initiated based on the theoretical analysis of Skoog and Askne [9]. The equipment was recently tested.

This paper will review recent developments of ground-based microwave radiometry. For further material, see [2], [10] and references contained within.

II. Basic Principles

A. Radiative Transfer

An absorbing material like the atmosphere emits blackbody radiation governed by Planck's law. At microwave frequencies and for tropospheric temperatures the Rayleigh–Jeans approximation to Planck's law can be used. The radiative intensity downwelling from the atmosphere and expressed in an equivalent brightness temperature T_B can be written as

$$T_B = T_{bg} \exp\left[-\int_0^\infty a(h')\,dh'\right] + \int_0^\infty T(h)\,a(h) \cdot \exp\left[-\int_0^h a(h')\,dh'\right] dh \quad (1)$$

Manuscript received September 12, 1985. The portions of this work done at the Chalmers University of Technology were supported by the Swedish Board for Space Activities and the Swedish Space Company.

J. I. H. Askne is with the Department of Electron Physics and the Onsala Space Observatory, Chalmers University of Technology, 412 96 Göteborg, Sweden.

E. R. Westwater is with the NOAA/ERL/Wave Propagation Laboratory, Boulder, CO 80303.

IEEE Log Number 8607726.

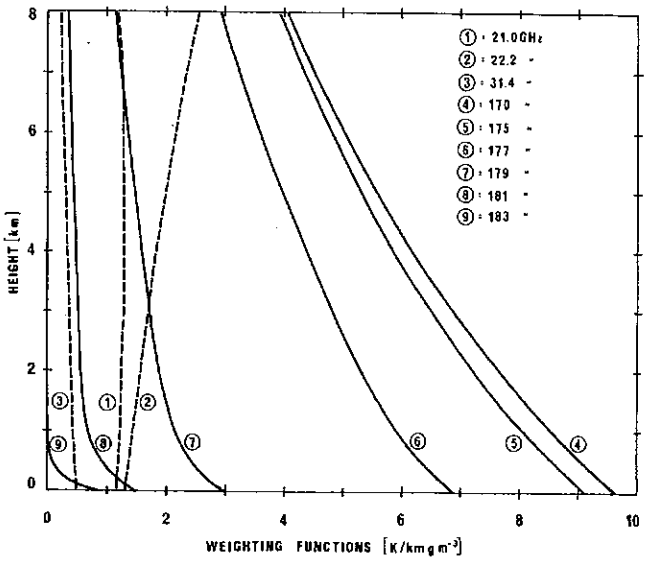

Fig. 1. Weighting functions of humidity in the zenith direction [22].

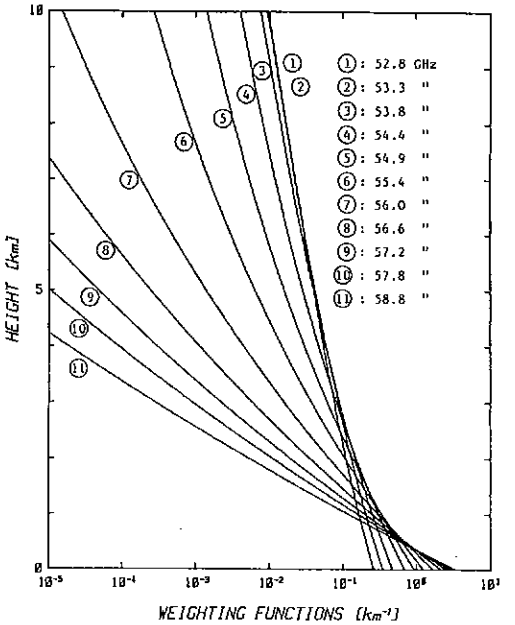

Fig. 2. Weighting functions of temperature for varying frequencies in the zenith direction [12].

where T_{bg} is the cosmic background radiation. The attenuation coefficient a is a complicated function of atmospheric temperature, pressure, water vapor, liquid water, and rain [11]. Water vapor has resonance lines at 22.2 and 183 GHz and oxygen has lines at 60 and 119 GHz. Changes in humidity and temperature are most easily detectable through measurements around these frequencies.

The radiation is a nonlinear function of the required quantities and we linearize the expression around a suitably chosen first guess, such as a climatological mean. We describe changes in the brightness temperature around the first guess by means of weighting functions which express the sensitivity of T_B to the variation of the humidity [7], $\Delta a(h)$, or the temperature [12] $\Delta T(h)$ around their initial values

$$\Delta T_b = \int_0^\infty [W_H(h, f, \theta)\, \Delta a(h) + W_T(h, f, \theta)\, \Delta T(h)]\, dh \quad (2)$$

for a certain frequency f and elevation angle θ. The weighting functions for humidity W_H and temperature W_T are illustrated in Figs. 1 and 2. These weighting functions are determined from expressions for the attenuation coefficient and some uncertainties still exist in these expressions. By discretization of (1) and (2) we obtain

$$\bar{g} = A\bar{f} \quad (3)$$

where $\bar{g}$ is the measurement vector containing the n physical measurement and the profile is represented by the vector $\bar{f}$. A is the matrix representation of the relevant weighting function. To this expression should be added the errors caused by experimental noise, by the discretization as well as by errors due to unknown properties of the atmosphere.

B. The Inverse Problem

Fig. 1 demonstrates that the sensitivity in the measurements to variations of water vapor around the mean value is almost constant with height at a frequency of 21.0 GHz. Observations at this frequency then yield a good estimate of the integrated water vapor through the atmosphere. This can be used in connection to astronomy or space applications to correct for phase delay and attenuation in the atmosphere. However, corrections have to made for cloud liquid water through observations at another frequency in the atmospheric window around 35 GHz. Observations are reported in [8] where the following formula for the integrated precipitable water vapor was derived from simultaneous observations with readiosondes:

$$V = -0.60 + 0.800T_b'(21) - 0.358T_b'(31.4)(\text{mm}) \quad (4)$$

where brightness temperatures corrected for "saturation" are used. Another possibility would have been to use adaptive retrieval coefficients [3]. A similar formula can be derived for cloud liquid, which yields an accuracy of 0.1 mm [3].

To derive profiles of atmospheric variables such as temperature and humidity, we face another problem. From Figs. 1 and 2 we see that the weighting functions do not provide a complete description of height variations and that any variation in the atmosphere which is orthogonal to the weighting functions can never be observed with the radiometer.

Mathematically this leads to an ill-posed inverse problem that would cause instability in a straightforward inversion algorithm. In order to determine profiles of humidity and temperature we must add further information to make possible an inversion of (1). A generally accepted

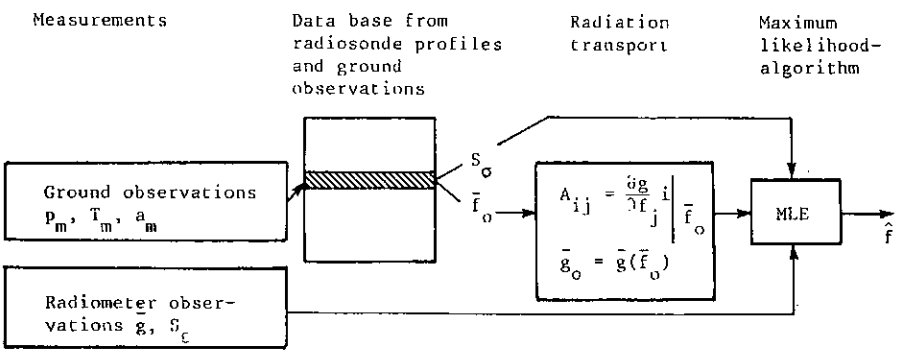

Fig. 3. Principal description of inversion method.

method is to apply constraints based on previous RAOB's [13], [14]. These previous observations can also be regarded as "virtual" measurements [14] at high resolution but with relatively high noise.

We now end up with an estimation problem which can be divided into two steps; see Fig. 3. First, the correlation between meteorological ground value and the profile values as a function of height is determined using minimum-variance estimation [15]. This allows us to use a more accurate estimate of the profile as an initial guess than the *a priori* mean. We chose a small part of the data base consisting of previous radiosoundings and derive a conditional mean $\bar{f}_0$, a value $\bar{g}_0$ calculated from $\bar{f}_0$, and a corresponding covariance matrix S_a. The calculation of the weighting coefficients is made for the initial guess of the profile, which reduces the non-linear effects. Second, the sensitivity of the brightness temperature for changes around the initial profile is calculated and finally a maximum likelihood algorithm determines the most probable profile taking into account all the observations with their uncertainties. The minimum-variance estimation of the profile is given by [13], [14], [7]

$$\hat{f} = \bar{f}_0 + (A^T S_\epsilon^{-1} A + S_a^{-1})^{-1} A^T S_\epsilon^{-1} (\bar{g} - \bar{g}_0) \quad (5)$$

where S_ϵ is the covariance matrix of the measurement errors. The covariance matrix for the estimated profiles is given by

$$\hat{S} = S_a - S_a A^T (A S_a A^T + S_\epsilon)^{-1} A S_a$$
$$= (A^T S_\epsilon^{-1} A + S_a^{-1})^{-1}. \quad (6)$$

From this constrained inversion method we obtain the expected rms error between retrieved and true profiles given by the diagonal elements of $\hat{S}$ in (6). In Fig. 4, we show accuracy estimates derived using (6) for two sets of climatological statistics. First, we performed dependent-set estimation analysis on two years of RAOB data taken during May at Torslanda airport (50 km away from Onsala Space Observatory). For this set, and for the 11-channel system whose weighting functions are given in Fig. 2, we determined the expected rms accuracy in retrieving temperature as a function of height. The results, representing experimental noise levels of 0.5, 0.1, and 0.0 K, are shown in Fig. 4(a)–(c). Curve *d* of this figure will be discussed in Section II-C. Using a similar climatology, simulations based on (6) were performed to estimate the accuracy in retrieving water-vapor profiles. These results, shown in Fig. 5, compare accuracies predicted for a currently existing system (21, 31.4 GHz), with those achievable by adding three additional channels located near the 183-GHz H_2O line.

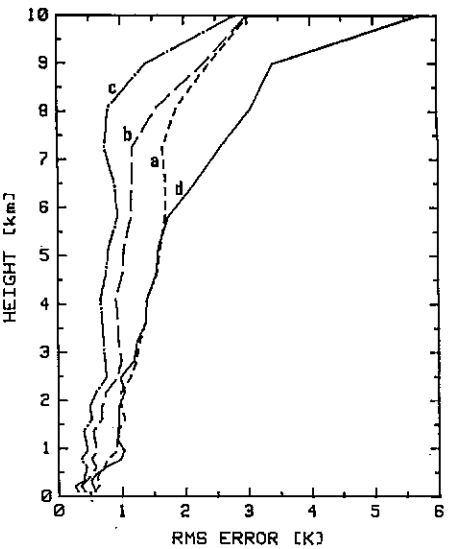

Fig. 4. Expected accuracy of retrieved temperature profiles. Curves *a–c*: Statistical inversion theory, Torslanda statistics (122 profiles). Curve *a* (- - -) 0.5 K, curve *b* (— —) 0.1 K, and curve *c* (- · -) 0.0 K radiometer accuracy. Curve *d* (——): Computer simulations, 83 ONSAM-profiles, Torslanda statistics, 0.5 K accuracy.

Some comments can be given about the computational problems:

To minimize the computing time it is important to use the most efficient representation possible for the profile. The profile variations around the surface-correlated estimate are then described by an empirical orthogonal function (eof) expansion rather than by the profile value at certain heights. These functions are derived by the surface-correlated estimate. By using the first six eof's, 98 percent of the profile variance of the statistical ensemble is covered. Since functions of higher order than six are excluded from the analysis, it is not possible to describe the very small-scale structure of the profiles. However, such variations are not detectable by our measurements.

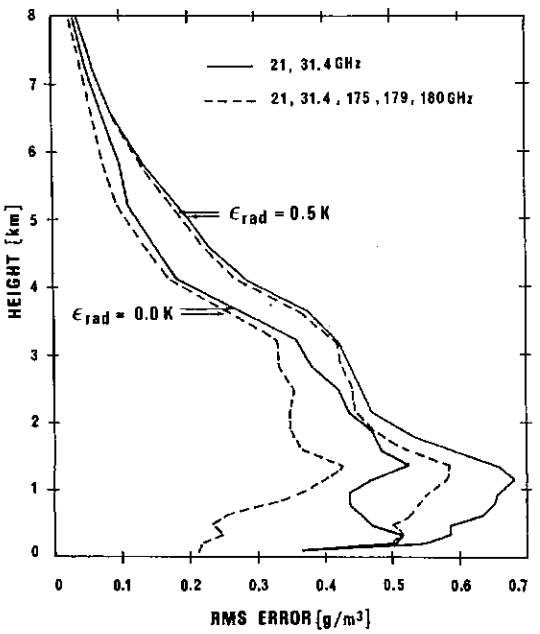

Fig. 5. Expected accuracy of retrieved water vapor profiles with statistical inversion theory [22].

The profile estimation (5) may be carried out sequentially [14] by using the observations one after the other. We may then correct for some of the non-linear effects by using the most linear measurements, i.e., the highest frequencies in the case of the temperature profiling radiometer, first and by correcting the weighting function in each step.

The accuracy of the retrieved profiles is critical for some meteorological applications and efforts are needed to increase the accuracy still more. As we discuss in Section IV, improvements can be made by combining ground-based observations with those from satellites, and by combining active and passive techniques. Another possibility arises due to the fact that the observations are taking place at close intervals. We may then use a Kalman filter algorithm to produce optimal estimates using the entire history of observations in the inversion process [16], [17]. As an extra constraint we use a description of the profile variation in time described by large-scale variations, $\phi(t, t+1)$, and a noise process $v(t)$

$$\bar{f}(t+1) = \phi(t, t+1)\,\bar{f}(t) + \bar{v}(t) \tag{7}$$

which gives rise to a similar expression for the measurable quantities

$$\bar{y}(t+1) = \Phi(t, t+1)\,\bar{y}(t) + \bar{\delta}(t). \tag{8}$$

The covariance matrix of the estimate can now be determined, and instead of (6) we obtain in principle

$$\hat{S}(t) = (A^T S_\epsilon^{-1} A + S_a^{-1} + A^T P(t)^{-1} A)^{-1} \tag{9}$$

where P is the prediction error covariance matrix based on the measurements. Equation (9) differs from the expressions in [14] as the filtering is made in the measurement space rather than in the profile space. This implies that the constraints given by the prediction become weaker but we use a more appropriate method, since the entire profile is not observable by the true measurements. From (9) we recognize the contributions from the measurements, the surface data constraints and the constraints due to previous measurements and so the roles of radiative transfer, statistical theory, and atmospheric dynamics are easily identified. However, it should be stressed that the constraints must be chosen with great care because their role can be as important in the profile estimation as the real measurements are. If we correctly describe the dynamical process in the atmosphere between two consecutive observations, we will obtain an accuracy that will approach the case of a radiometer with infinite accuracy; see Fig. 4, curve *c*, and Fig. 5. In practice, however, this accuracy can never be reached. The most severe problem may be non-Gaussian noise characterizing the radiometer accuracy.

C. Computer Simulations

Some important aspects of the constrained inversion method can only be studied by computer simulations as illustrated in Fig. 6. The maximum likelihood algorithm is based on the assumption that the observed profile is part of the statistical ensemble. However, that is not always the case as the observations do take place at times or even places other than those where the radiosoundings have been performed. The effects of this can be tested by the method illustrated in Fig. 6. We have studied two cases during a recent experiment, the so called ONSAM experiment (Onsala Atmospheric Measurements, Onsala Space Observatory, May 2–26, 1983). One of the aims of this experiment was to test the accuracy of a new temperature-profiling radiometer. In the test, two years of radiosonde data during the month of May from Torslanda airport (50 km away from the observing site) were used as the statistical data base in the inversion theory.

During the ONSAM experiment, 81 radiosondes were launched. We now determine the corresponding theoretical brightness temperature, add noise, and retrieve profiles based on the Torslanda statistics. The result is illustrated in Fig. 4, curve *d*, and an important difference is obtained above 6 km due to a difference between true and virtual observations. Besides the rms difference, we will find that we have a mean difference between true and retrieved profiles. This difference is found to be almost the same as the difference between the mean profile from Torslanda and the mean profile during the ONSAM experiment. In Fig. 4, curve *d*, we particularly note the clear difference at the tropopause height.

It is apparent that good statistical background information may be crucial for obtaining the kind of accuracy needed for some meterological applications. We should thus provide optimum *a priori* information by using both physical constraints and judicious meteorological information.

The accuracy of the radiometer can be tested by the simulation method and we then find [18], [19] that if the

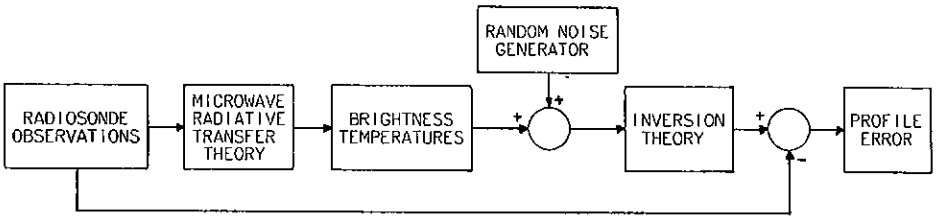

Fig. 6. Computer simulations of retrieval process.

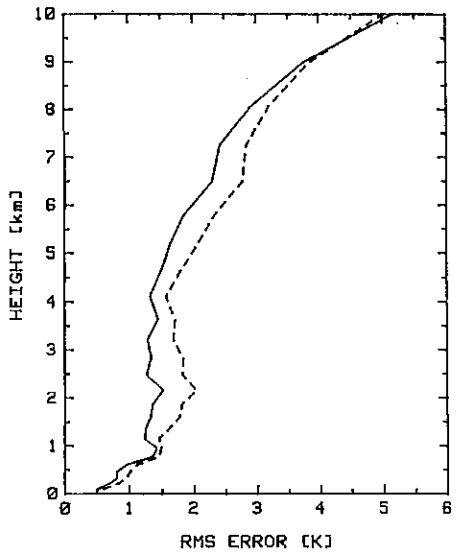

Fig. 7. rms error of retrieved temperature profiles during clear-sky and cloudy conditions, 28 profiles, 4 channels (- - - -), and 11 channels (——).

absolute accuracy of the radiometer is increased to 0.1–0.2 K the accuracy of the retrieved profiles in practice, would not increase due to incompatibility between true and virtual observations. In general, the accuracy is determined by the largest source of noise, whether it be from instruments, virtual observations, or emission from contaminants, such as clouds.

The value of using eleven frequencies rather than four in the temperature profiling case can be tested by redoing the inversion based only on the relevant four channels. The result is illustrated in Fig. 7 and we can conclude that the result agrees with the theoretical analysis [9], [19].

D. Height Resolution of the Profiles

An important point is the vertical resolution of the profiles. From the weighting functions we conclude that the height resolution from the radiometer observations is far from being as good as that from radiosondes. On the other hand, information from previous radiosondes is included in the retrieved profiles, and the question is how to estimate objectively the effective height resolution. This has been discussed by Rodgers [20].

III. Design of the Radiometers

In this section, we will briefly describe the radiometers used by CUT and those used by NOAA. A complete description of these instruments is given in [2], [7], and [19].

TABLE I
Center Frequencies for Channels Used in the NOAA Profiler Radiometric System [2]

Channel	Frequency	Atmospheric constituent most effective	Bandwidth (GHz)
1	20.60	water vapor	1.0
2	31.65	liquid	1.0
3	52.85	temperature	0.1
4	53.85	temperature	0.1
5	55.45	temperature	0.1
6	58.80	temperature	0.1

The designs of the water-vapor radiometers at NOAA and CUT are somewhat different. This is even more the case for the temperature-profiling radiometers. In the latter case, the goal for the CUT design was to build a low-cost radiometer by sacrificing the possibility to measure at all the frequencies at the same time. On the other hand, the aim was to increase the accuracy by measuring at several frequencies (eleven) and using a low-temperature reference load (−21°C). The antenna consists of a conical horn with a beamwidth of 6°, the same as used for the water-vapor radiometer. In contains a dielectric ring designed to suppress sidelobes and give the antenna pattern a Gaussian shape. The calibration of the radiometer was performed by measuring the signals from absorbers kept at room temperature and liquid nitrogen as well as measurements during clear-sky conditions when the brightness temperature can be calculated from radiosonde data. Studies of 13 radiosonde profiles reveal an rms difference between the calculations and the observations of less than 0.5 K, accepting an offset due to uncertainties in the absorption coefficients. This offset was 2.4 K at the lowest frequency, 1.8 at the next lowest, and not larger than the rms uncertainty at the other frequencies. This would correspond to an uncertainty of less than 3 percent in the attenuation coefficient.

The NOAA Profiler radiometer is a six-channel instrument, whose frequency and bandwidth characteristics are given in Table I. The Profiler observes zenith radiation with equal beamwidths of 2.3° at all channels. All measurements are simultaneous with 2-min averages of brightness temperature being retained for further processing. Calibration of the two water channels uses the tipping curve method [3], while calibration of the temperature channels depends on brightness temperatues calculated from RAOB's. In general, the differences between measured and calculated brightness temperatures are around 0.5 to 1.0 K rms.

IV. Observational Results

A. Water Vapor

It is well known that precipitable water vapor V can be accurately measured by dual-channel microwave radiometers [3]. The rms accuracy in deriving V is about 1.0 to 1.5 mm and is comparable to that obtained from radiosondes. The excellent temporal resolution (~ 1 min) of these determinations of V is sufficient for applications in long baseline radiointerferometry and geodetic metrology [8], [21]. In addition, these measurements may have application to precipitation and weather forecasting.

It would be highly desirable if water vapor profiles could be derived from the radiometric measurements. Given that surface measurements of absolute humidity are available, vapor profiles can be derived from dual-channel observations [3], [7]. The accuracy of vapor profiling has been evaluated experimentally using the CUT radiometers [7], [22] and also using the NOAA Profiler [23]. The results from these two instruments, shown in Fig. 8 for the CUT and in Fig. 9 for the NOAA Profiler, are similar. Fig. 9(c), comparing dual-channel versus Profiler retrievals shows that adding the temperature channels to the vapor retrieval adds very little information.

Plots of individual retrievals [7], [23] show that the vertical resolution of the retrieved vapor profiles is poor, and sharp changes in profiles are not recovered. Thus, these coarse vertical resolution profiles are clearly not adequate for some meteorological purposes. However, limited use can be made of the profiles in 1) correction of electrical path fluctuations due to water vapor for systems that rely on the measurement of phase of radio waves originating outside the atmosphere, 2) radiometric determination of pressure heights, 3) corrections to radiometric determination of temperature profiles, and 4) corrections for attenuation and emission due to water vapor (e.g., infrared measurements can be corrected for water vapor using profile information derived from microwaves).

The water-vapor profiling capability could be improved by using a multifrequency system that includes observations at frequencies in the 140–183 GHz range. According to a simulation study the profiling accuracy was shown to improve 20 percent in low layers by including three frequencies at 175, 179, and 180 GHz [22]. Observational results using 21.5 and 176 GHz of similar type were reported in [5].

B. Temperature

The 11-channel CUT radiometer was operated in the ONSAM field experiment, in which RAOB soundings were also available. In this experiment, 13 radiosonde observations were taken during clear-sky conditions. These observations were compared with 50 simultaneous radiometer measurements and the rms difference between the radiosonde data and the retrieved profiles is illustrated in Fig. 10, curve *a*. We conclude that the difference between this curve and the simulated curve *d* of Fig. 4 is rather small. It should be stressed at this point that the only possible way to test the profiles derived from the microwave radiometers is by comparison with radiosondes. However, the radiosonde takes about half an hour in ascent to tropopause height during what time the balloon may well have drifted many tens of kilometers sideways. This is in contrast to the radiometers that perform an observation in seconds or minutes and are sensitive to an airmass with an extent of less than 1 km at 10 km height. Furthermore, the accuracy of the sensors on the radiosondes vary.

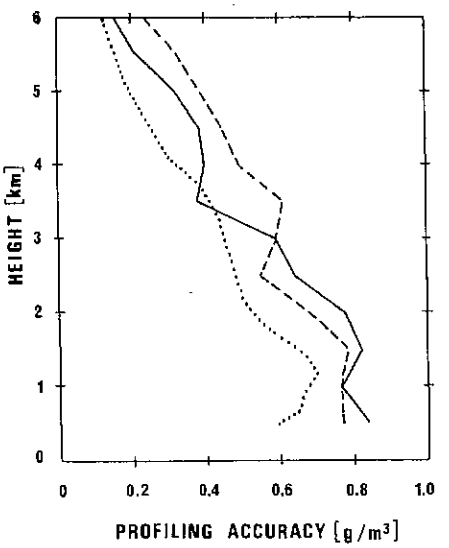

Fig. 8. rms errors of retrieved water vapor profiles during clear-sky, 22 profiles (——), and cloudy conditions, 16 profiles (- - - -). Theoretical expected accuracy (- - - -) [7], [22].

When clouds are present, correction must be made to ther water-vapor radiometer data. In order to do this the equivalent clear-sky brightness temperature of each channel is predicted by adding corrections linearly related to the brightness temperatures at 21.0 and 31.4 GHz. The coefficients were derived by statistical linear regression based on a set of cloud models and an expression for the cloud liquid absorption coefficient [19]. This correction algorithm is applied as soon as the water-vapor radiometer yields a liquid water output larger than its rms accuracy. The accuracy of the retrieved profiles is now determined by the water-vapor radiometer (with an absolute accuracy of 1 K) as well as the temperature-profiling radiometer and thus a degradation of the accuracy is introduced compared to the clear-sky case as illustrated in Fig. 10.

During the ONSAM experiment the water-vapor radiometer and the temperature-profiling radiometer were placed 500 m apart and not perfectly time synchronized. The two radiometers were then not observing the same air-mass, which is very important when making cloud corrections. Meaningful results could then only be obtained during stable conditions. These results compared with 15 radiosonde measurements are illustrated in Fig. 10, curve *b*. Some retrieved profiles from May 17, 1983 are illustrated in Fig. 11, including one derived from a NOAA-7 passage.

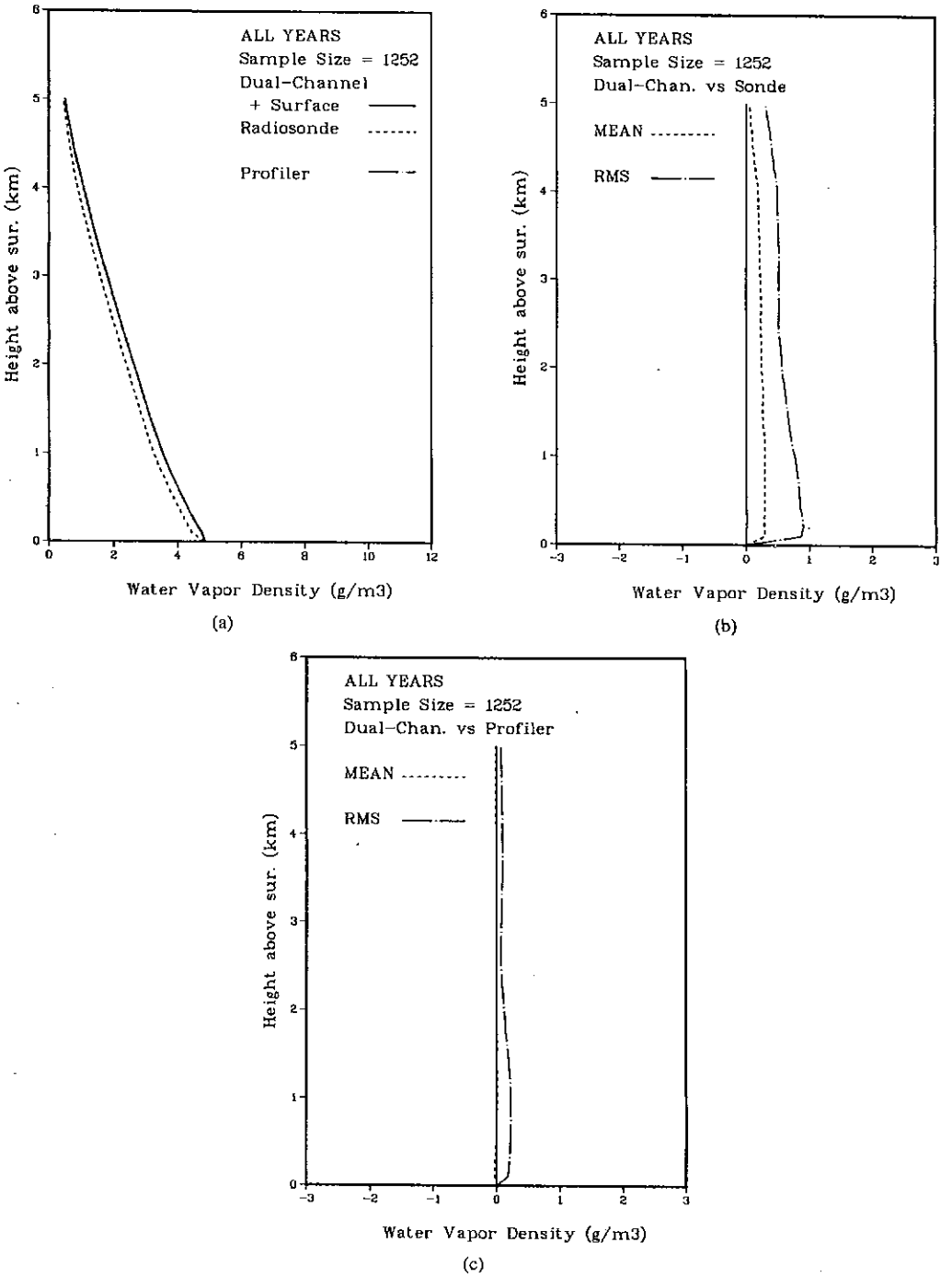

Fig. 9. Statistical comparisons of Profiler radiometric retrievals with RAOB's for the years 1982–1983 [23].

These retrievals are typical and illustrate some general features of ground-based radiometric retrievals. The gross characteristics of the profiles are well represented up to tropopause altitudes. In fact, up to about 500 mbar, such integrated quantities as pressure heights and thicknesses are determined with an accuracy approaching that of RAOB's [1]. However, Fig. 11 illustrates a problem with the radiometer—the tendency to smooth the profile so that information about elevated inversion layers is lost. It may be possible that information from active sensors, such as radar or lidar, can improve the retrievals at such critical points. Another possibility is elevation angle variation to yield information on inversion layers at low altitudes.

The NOAA Profiler has been operated at Stapleton International Airport, Denver, Colorado, for about two years. The radiometers are located less than 50 m from the National Weather Service RAOB release facility, and the twice-a-day RAOB's are available for "ground truth."

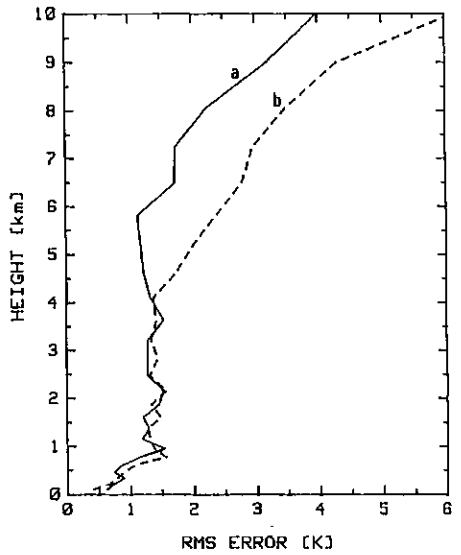

Fig. 10. Comparison between retrieved and radiosonde profiles under clear-sky conditions, 13 profiles, curve a (——) and cloudy conditions, 15 profiles, curve b (- - - -).

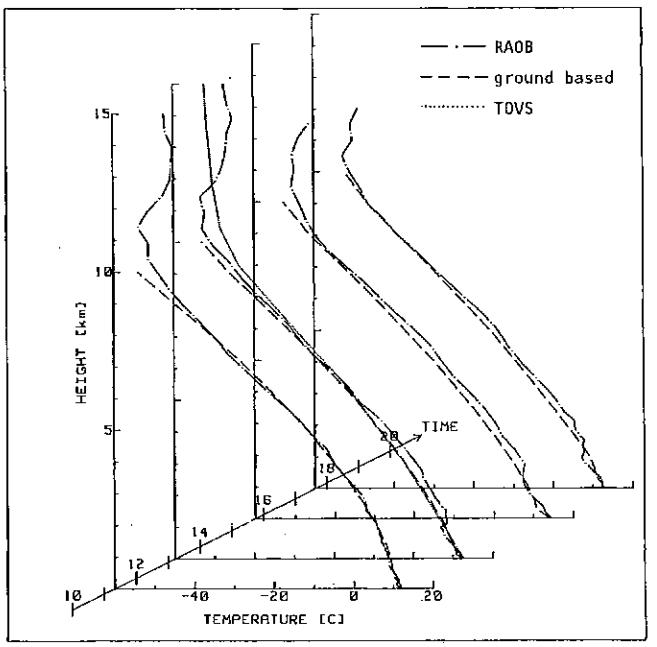

Fig. 11. Demonstrating some profiles derived during the ONSAM experiment. (- · -) RAOB, (— —) profile derived from ground-based radiometer, and (.....) from TOVS.

In Fig. 12 we show the mean and rms differences between Profiler and RAOB determinations of the mean temperature for 100-mbar layers [24]. These data are based on 255 cases, March through July of 1982. For comparison, we also show the *a priori* prediction of retrieval error. The close agreement between predicted and achieved accuracy suggests that confidence may be placed in simulations of system performance.

A time sequence of temperature retrievals, extending over 14 h, is shown in Fig. 13 [2]. Although some of the

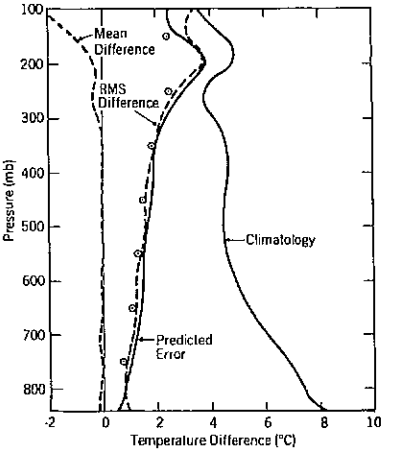

Fig. 12. Predicted radiometer temperature errors (solid lines) and observed differences between radiometer and radiosonde (dashed lines). Circles are rms differences of radiometer and radiosonde 100-mbit layer mean temperatures [24].

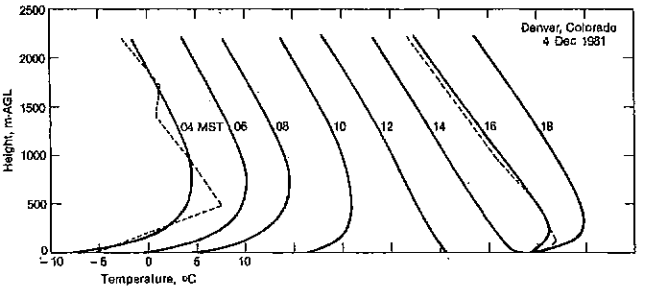

Fig. 13. Time sequence of lower atmosphere temperature profiles at 2-h intervals showing decay and reformation of ground-based temperature inversion. Successive profiles are displaced by 5° to the right of the preceding profile. Dashed lines are radiosonde profiles at 0400 MST [2].

sharp profile structure is smoothed, a reasonable representation is obtained of the decay and reestablishment of the nocturnal thermal inversion.

C. Measurements of Cloud Liquid

Cloud liquid is usually viewed as a contaminant on the microwave radiometric determination of temperature and water vapor. However, measurements of liquid are turning out to be valuable in their own right. For example, to warn aircraft pilots of possible icing conditions, microwave measurements of super-cooled liquid show promise [25]. In addition, the use of microwave radiometry in weather modification has been documented [26]. In this section, we will discuss ground-based techniques for radiometric determination of cloud liquid.

One technique used to determine integrated cloud liquid L is identical in form to that described by (4) to derive precipitable vapor V. Another technique is to first derive attenuation from emission measurements of T_b. Then, using T_b measurements at two properly chosen vapor and liquid sensitive frequencies, L is derived [27]. A statistical algorithm is also possible, but since neither L nor profiles of liquid density are measured by RAOB's, modeling must be done to develop satisfactory *a priori* data [28].

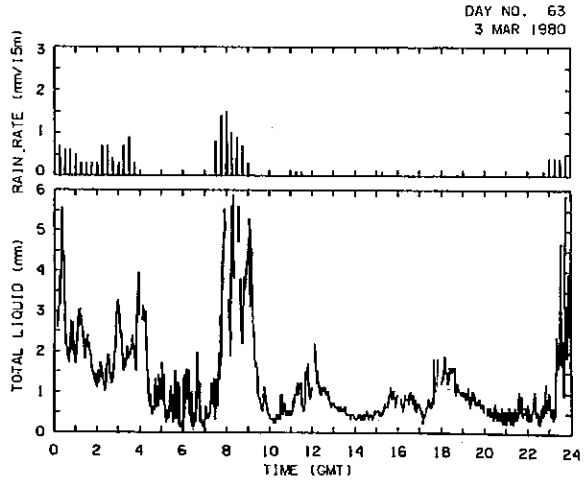

Fig. 14. Total path liquid measured by the radiometric system on March 3, 1980. Rainfall data were measured at the radiometer site using a weighing bucket raingage [26].

Since RAOB's do not measure L, ground-truth measurements to verify the accuracy of the radiometric determination are very difficult to obtain. Probably the best comparison to date is that of Snider *et al.* [35]. They compared liquid, determined from the absorption of a microwave satellite signal, with radiometrically measured liquid, and found rms differences of 0.28 mm. Theoretical predictions, valid for nonprecipitating clouds, indicate that about 10-percent accuracy in the determination of L can be achieved.

As an example of the kind of liquid data produced routinely by a dual-channel system, we show in Fig. 14 a time series of data measured during a cloud-seeding experiment [26]. As might be expected, a high degree of temporal variability is present in the behavior of L.

A two-frequency microwave radiometer with a fully steerable antenna has also shown some interesting angular variations in both integrated vapor V and liquid L. In Fig. 15 are shown data obtained by scanning a dual-channel system at a constant elevation angle of 15° [29]. Such data may be useful for determining departures from stratification of V on radio phase measuring systems and in determining concentrations of liquid in visually homogeneous clouds.

V. Ground-Based Radiometers Combined with Other Instruments

A. Combined Ground-Based and Satellite Sensing of Temperature Profiles

Because of the decay with altitude of ground-based weighting functions, it becomes increasingly difficult to achieve useful accuracies at heights above, say, 5 km above the surface. However, an attractive source of complementary data is available from satellites. For example, microwave and infrared brightness temperatures are available at least twice-a-day from each of two NOAA polar-orbiting satellites. In this section, we briefly summarize

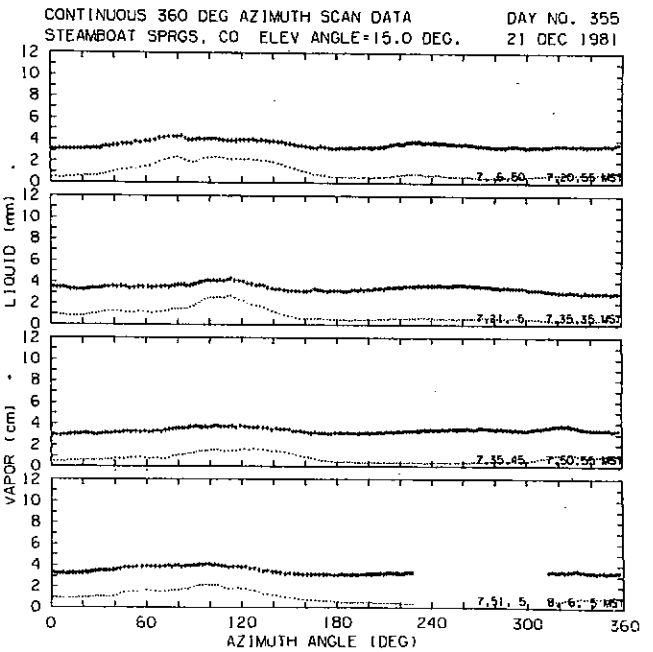

Fig. 15. Radiometer output during a series of azimuth scans at 15° elevation angle [29].

experimental results of combining ground- and satellite-based microwave radiometers.

Remote sensing of temperature profiles using a combination of passive microwave radiometric observations from surface- and satellite-based platforms was suggested by Westwater and Grody [30]. Their computer simulations showed that over the pressure interval 1000–300 mbar, rms retrieval accuracies of 1–2°C were achievable with current radiometric technology. Such simulations were based on (6) in predicting the performance of different combinations of remote-sensing systems. These simulations predicted that the surface-based radiometers would yield significantly better accuracy than the satellite in the first 300 mbar above the surface, the satellite is the more accurate of the two above this level, and the combination of the two is a significant improvement over either separate system.

Both of the experimental systems described in Section III are now available to allow the combination of ground- and satellite-based observations. In particular, data from the ground-based Profiler [2] and the orbiting satellite-based Microwave Sounding Unit (MSU) [31] have been used for this combination. The MSU is a component of an operational sounding system and was designed 1) to produce global temperature soundings under nearly all weather conditions, and 2) to complement an infrared sounder that contains more channels but is limited to clearer atmospheres. The MSU is aboard the polar-orbiting NOAA-6, -7, -8 satellites and contains four channels in the oxygen band, at 50.30, 53.74, 54.96, and 57.95 GHz, to provide temperature profile information from the lower troposphere to the lower stratosphere. Only the upper three channels are used for temperature sensing. Further details of this instrument, including its scan pattern,

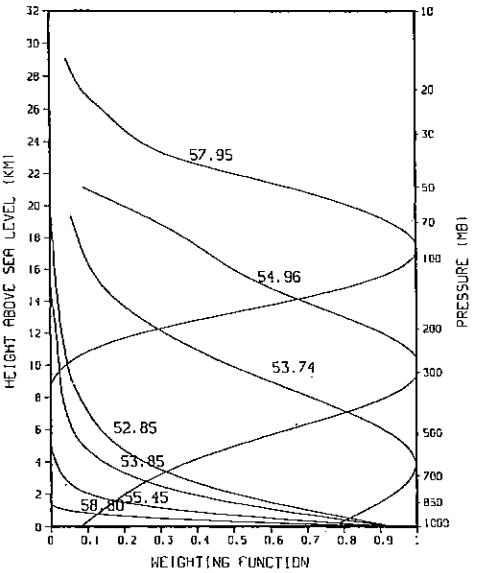

Fig. 16. Temperature weighting function, in relative units, for various channels of the radiometric Profiler and the MSU. The upper three curves are for the MSU; the lower four curves are for the Profiler [32].

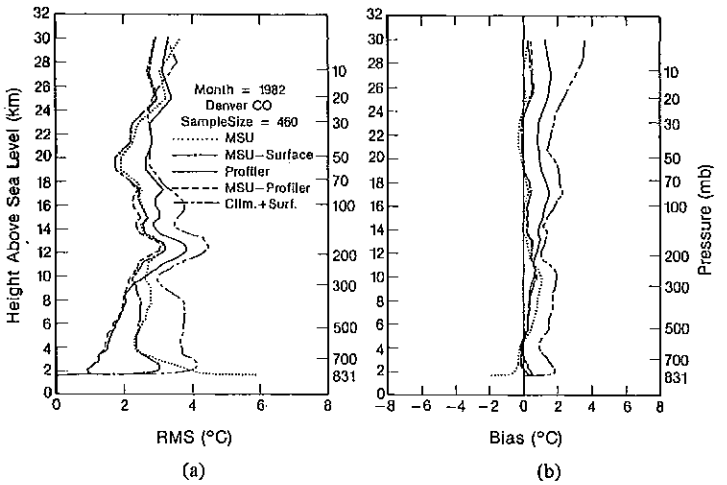

Fig. 17. Statistics of differences between RAOB's and retrievals: (a) total rms differences; (b) biases. Bias refers to RAOB retrieval [32].

are given by Grody [31]. Profiler and MSU temperature weighting functions are shown in Fig. 16. Note how the Profiler capabilities, which are exponentially reduced above 500 mbar, are complemented by the MSU; conversely, note how the relatively high vertical resolution at lower altitudes of the Profiler complements the MSU below 500 mbar.

Data from the Profiler and the MSU were collected over Denver, Colorado, for about one year [32]. As a standard with which to compare retrievals, National Weather Service RAOB's were also obtained. For the time period December 1981 through December 1982, 460 RAOB–Profiler–MSU data cases were obtained. From these data, temperature profiles were derived using data from the 1) Profiler; 2) MSU; 3) MSU with surface meteorological measurements; and 4) Profiler with MSU. The total rms difference statistics relative to RAOB's, for each of the four temperature retrievals, are shown in Fig. 17. As a baseline value, the rms variation is shown using surface meteorological measurements as predictors. Note that the MSU with Profiler results are everywhere more accurate than any of the separate subsystems. This result was both expected and desired, but if relative covariances had been modeled incorrectly, for example, combined retrievals might be poorer than the separate ones. We also observe that the retrieval results of all the systems improved substantially over predictions based on surface climatology, except for the MSU in the first 50 mbar above the surface.

Pressure heights and thicknesses were also derived from the combined Profiler–MSU data [32]. The accuracy of these quantities was shown to be approaching the functional precision of National Weather Service RAOB's.

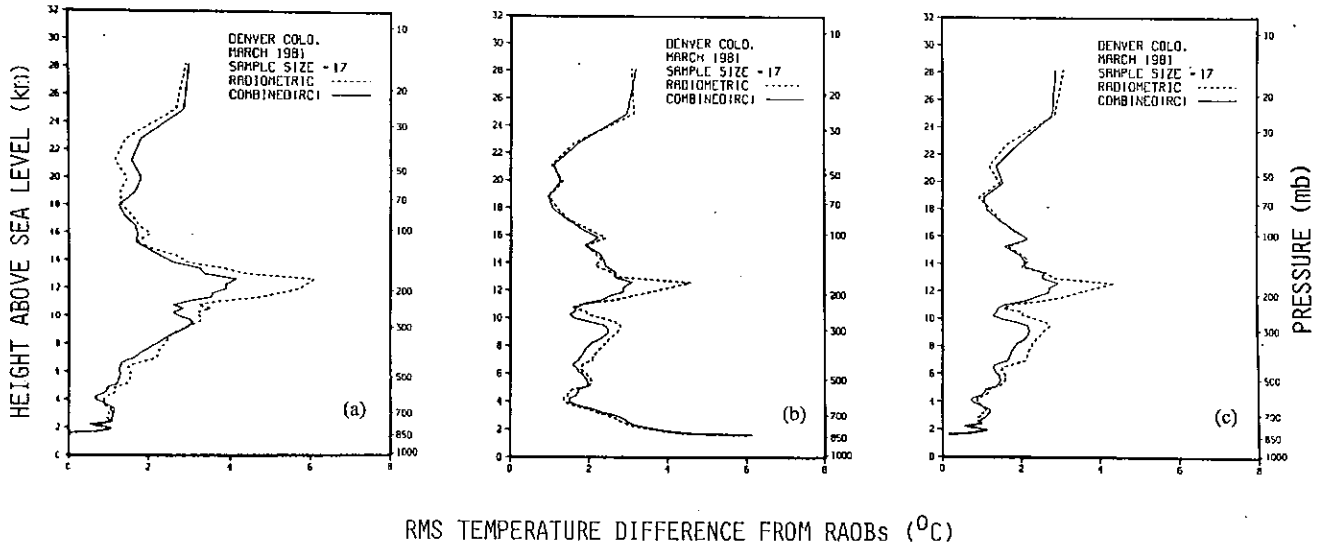

Fig. 18. The rms differences between temperature retrievals and NWS RAOB's Curves labeled "combined" refer to radiometer + radar data. (a) Profiler + VHF radar; (b) MSU + VHF radar; (c) Profiler + MSU + VHF radar [32].

B. Combined Radar-Radiometric Temperature Retrievals

Studies have shown that VHF radars can measure the height of the tropopause [33]. As predicted theoretically by Westwater and Grody [30] and verified experimentally [34], the tropopause height information can be used to improve temperature retrieval accuracy of radiometric sensors. In this section, we will show examples of the combined passive–active techniques for a small data set taken during March 1981. Details of the VHF radar and the processing techniques used to derive tropopause height are given in [34].

In [32], temperature retrievals were combined for three passive systems (Profiler, MSU, and Profiler with MSU) and three passive plus active systems (each passive systems plus VHF radar). The retrieval algorithms used to incorporate active and passive measurements is a straightforward generalization of (5) and is described by Westwater *et al.* [34].

The rms differences for the three combinations are shown in Figs. 18(a)–(c). Fig. 18(a) shows ground-based radiometer and VHF radar. Note the large improvement in retrieval accuracy, ~ 2-K rms, near tropopause pressures (300 to 100 mbar), when tropopause height measurements are added. However, retrieval accuracy above 300 mbar is poor.

Fig. 18(b) shows satellite-based radiometer (MSU) plus VHF radar. Again, note ~ 2-K rms improvement of MSU results when the tropopause height measurements are inserted. Here, retrieval accuracy below about 700 mbar ranges from almost 3- to 6-K rms.

Fig. 18(c) shows ground-based radiometer plus VHF radar plus MSU. The solid curve, representing the combined radiometric systems, shows improvement over either of the pure radiometric results of Fig. 8(a) or (b), except in the vicinity of the tropopause. A further increase in accuracy is achieved by adding the radars measurement of tropopause height, as shown by the dashed curve in this figure. Except for a narrow pressure region near 200 mbar, the rms differences from the surface to 30 mbar are less than 2 K.

VI. Discussion

In order to further develop ground-based microwave radiometers for general meteorological use it is important to 1) make observations under different meteorological conditions; 2) test different technical systems; and 3) improve the vertical resolution of the retrieved profiles.

In this paper results of two ground-based microwave radiometric systems have been reviewed: the new temperature-profiling radiometer tested in the ONSAM experiment and the NOAA Profiler. General conclusions are that:

1) Observations at 11 frequencies yield a better result than observations at only 4.
2) As expected, it is very important to observe the same air mass with the water-vapor and temperature-profiling radiometers.
3) Good *a priori* data can be crucial in obtaining accuracy for some meteorological applications.

In order to use the potential offered by ground-based microwave radiometry, forecasting and nowcasting methods have to be developed taking into account the possibilities of almost continuous profiling or at least updating of the forecast at optimal times rather than specific times as mandated by worldwide agreement.

The advantages of being able to measure almost continuously are hard to evaluate before sufficient experience has been gained. But it may well be that short-time and

small-scale motions of the atmosphere may develop to large-scale motions and that microwave radiometry will prove valuable in improving forecasts in more than one way.

A network of ground-based microwave radiometers and VHF radars can be combined with satellites to form a meteorological observing system that provides both temporal and spatial information on temperature, moisture, and winds. The potential information context of such a system of complementary observations is enormous.

Dual-channel radiometers will continue to be useful in geodetic metrology, long-baseline interferometry, weather modification experiments, etc. Coupled with wind-sensing radars, a system to measure flux of vapor could be developed.

In general, as we develop more precise instruments and better ways of combining existing observing systems, we will improve both our knowledge of atmospheric phenomena and the physical mechanisms underlying the techniques of remote sensing.

Acknowledgment

J. Askne would like to express his gratitude to G. Skoog for discussions on Kalman filtering.

References

[1] E. R. Westwater *et al.*, "Determination of atmospheric temperature profiles from a statistical combination of ground-based Profiler and operational NOAA 6/7 satellite retrieval," *J. Climate Appl. Meteor.*, vol. 23, pp.689–703, 1984.

[2] D. C. Hogg *et al.*, "An automatic profiler of the temperature, wind and humidity in the troposphere," *J. Appl. Meteor.*, vol. 22, pp. 807–831, 1983.

[3] D. C. Hogg *et al.*, "A steerable dual-channel microwave radiometer for measurements of water vapor and liquid in the troposphere," *J. Appl. Meteor.*, vol. 22, pp. 789–806, 1983.

[4] Z. Bolin *et al.*, "The principle and tests of microwave remote sensing atmospheric sounding," *Scientia Sinica*, vol. XXIV, pp. 363–373, 1981.

[5] K. P. Gaikovich *et al.*, "Investigation of remote sensing possibilities of the lower atmosphere in the microwave range and some aspects of statistical data use," *Int. J. Remote Sensing*, vol. 4, pp. 419–431, 1983.

[6] B. Schönwald and B. Pucher, "Bestimmung des Temperaturprofils in der atmosphärischen Grenzschicht durch bodengebundene Mikrowellen-Radiometrie," *Mikrowellen Magazin*, vol. 20, no. 8, pp. 92–95, 1980.

[7] G. Skoog *et al.*, "Experimental determination of water vapor with microwave radiometry," *J. Appl. Meteor.*, vol. 21, pp. 394–400, 1982.

[8] G. Elgered *et al.*, "Measurements of atmospheric water vapor with microwave radiometry," *Radio Sci.*, vol. 17, pp. 1258–1264, 1982.

[9] G. Skoog and J. Askne, "The capability of microwave radiometers for temperature profiling of the atmosphere," in *Proc. 12th European Microwave Conf.* (Sept. 13–17, 1982, Helsinki, Finland). Tunbridge Wells, U.K.: Microwave Exhibitions and Publishers LTD, 1982. pp. 95–100.

[10] F. T. Ulaby *et al.*, *Microwave Remote Sensing*, vol. III. Reading, MA: Addison-Wesley, to be published.

[11] H. J. Liebe, "Atmospheric EHF window transparencies near 35, 90, 140, and 220 GHz," *IEEE Trans. Antennas Propagat.*, vol. AP-31, pp. 127–135, 1983.

[12] G. Skoog, "Remote sensing of atmospheric humidity and temperature profiles by ground-based microwave radiometry," School of Elec. Eng., Chalmers Univ. Tech., Tech. Rep. 3L, 1983.

[13] E. R. Westwater and O. N. Strand, "Statistical information content of radiation measurements used in indirect sensing," *J. Atmos. Sci.*, vol. 25, pp. 750–758, 1968.

[14] C. D. Rodgers, "Retrieval of atmospheric temperature and composition from remote measurements of thermal radiation," *Rev. Geophysics Space Phys.*, vol. 14, pp. 609–624, 1976.

[15] R. Deutsch, *Estimation Theory*. Englewood Cliffs, NJ: Prentice-Hall, 1966.

[16] G. Skoog and J. Askne, "The Kalman filter applied to ground-based microwave radiometric sensing of atmospheric temperature profiles," in *Preprint Volume, Int. Geosci. Remote Sensing Symp.* (Aug. 31–Sept. 2, 1983, San Francisco), 1983.

[17] P. Basili, P. Ciotti, and D. Solimini, "Inversion of ground-based radiometric data by Kalman filtering," *Radio Sci.*, vol. 16, pp. 83–91, 1981.

[18] G. Skoog, J. Askne, and E. Winberg, "On the accuracy of temperature profiles measured by ground-based microwave radiometry," in *Preprint Volume, WMO Tech. Conf. Instruments and Cost-Effective Meterol. Observations* (Sept. 24–28, 1984 Noordwijkerhout, The Netherlands), pp. 223–226, 1984.

[19] J. Askne *et al.*, "Tests of a ground-based microwave radiometer for atmospheric temperature profiling with meteorological applications," *Int. J. Remote Sensing*, to be published.

[20] C. D. Rodgers, "The vertical resolution of remotely sounded temperature profiles with *a priori* statistics," *J. Atmos. Sci.*, vol. 33, pp. 707–709, 1976.

[21] D. C. Hogg, F. O. Guiraud, and M. T. Decker, "Measurement of excess ratio transmission length on earth-space paths," *Astron. Astrophys.*, vol. 95, pp. 304–307, 1980.

[22] J. Askne and G. Skoog, "Atmospheric water-vapor profiling by ground based radiometry at 22 and 183 GHz," *IEEE Trans. Geosci. Remote Sensing*, vol. GE-21, pp. 320–323, 1983.

[23] E. R. Westwater, M. J. Falls, and M. T. Decker, "Remote sensing of atmospheric water vapor by ground-based microwave radiometry," in *Proc. Moisture and Humidity 1985, Measurement and Control in Science and Industry* (Washington, DC, Apr. 15–19, 1985), to be published.

[24] M. T. Decker, "A comparison of radiosonde and radiometrically derived atmospheric observations," in *Proc. WMO/AMS/CMOS 5th Symp. Meteor. Observations and Instrumentation* (Apr. 11–15, 1983). Boston: Amer. Meteor. Soc., pp. 205–206.

[25] D. C. Hogg, F. O. Guiraud, and E. B. Burton, "Stimultaneous observations of cool cloud liquid by ground-based microwave radiometry and icing of aircraft," *J. Appl. Meteor.*, vol. 19, pp. 893–895, 1980.

[26] J. B. Snider and D. Rottner, "The use of microwave radiometry to determine a cloud-seeding opportunity," *J. Appl. Meteor.*, vol. 21, pp. 1291–1296, 1982.

[27] E. R. Westwater, "The accuracy of water vapor and cloud liquid determination by dual frequency ground-based microwave radiometry," *Radio Sci.*, vol. 32, pp. 677–685, 1978.

[28] M. T. Decker, E. R. Westwater, and F. O. Guiraud, "Experimental evaluation of ground-based microwave radiometric sensing of atmospheric temperature and water vapor profiles," *J. Appl. Meteor.*, vol. 17, pp. 1788–1795, 1978.

[29] J. B. Snider, "Observations of liquid water in orographic clouds using a steerable microwave radiometer." in *Preprint Volume, 5th Symp. Meteor. Observations and Instrumentation* (Apr. 11–15, 1983, Toronto, Ont.). Boston: Amer. Meteor. Soc., 1983, pp. 196–198.

[30] E. R. Westwater and N. C. Grody, "Combined surface- and satellite-based microwave temperature profile retrieval," *J. Appl. Meteor.*, vol. 19, pp. 1438–1444, 1980.

[31] N. C. Grody, "Severe storm observation using the Microwave Sounding Unit," *J. Climate Appl. Meteor.*, vol. 22, pp. 609–625, 1983.

[32] E. R. Westwater *et al.*, "Remote sensing of temperature profiles by a combination of ground-based Profiler and satellite-based MSU radiometric observations," in *Preprint Volume, Conf. Satellite/Remote Sensing and Applications* (June 25–29, 1984, Clearwater Beach, FL). Boston: Amer. Meteor. Soc., 1984, pp. 191–196.

[33] K. S. Gage and J. L. Green, "Tropopause detection of partial specular reflection with very-high-frequency radar," *Science*, vol. 203, pp. 1238–1240, 1979.

[34] E. R. Westwater *et al.*, "Ground-based remote sensing of temperature profiles by a combination of microwave radiometry and radar," *J. Climate Appl. Meteor.*, vol. 22, pp. 126–133, 1983.

[35] J. B. Snider *et al.*, "Comparison of cloud liquid content measured by two independent ground-based systems," *J. Appl. Meteor.*, vol. 19, pp. 577–579, 1980.

Jan I. H. Askne (S'63—M'65) was born in 1936. He received the Civilingenjör (M.Sc.) degree in electrical engineering in 1961 and the Ph.D. degree in 1970 from Chalmers University of Technology, Göteborg, Sweden.

Since 1961, he has been a member of the Research and Technical Staff of the Department of Radio and Space Science at Chalmers University of Technology and of the Onsala Space Observatory and he is presently Professor in Remote Sensing. He has published articles on wave progagation problems in complex media, radiation from molecules in cosmic clouds, and remote-sensing problems. His present research interest is mainly remote sensing of atmospheric properties by microwave radiometry but include as well oceanographic applications of microwave radiometry, altimetry, and scatterometry.

Ed R. Westwater was born on October 29, 1937, in Denver, CO. He received the B.A. degree in physics and mathematics from Western State College of Colorado in 1959, the M.S. degree in physics in 1962, and the Ph.D. degree in physics in 1970 from the University of Colorado.

He is currently employed as a Supervisory Physicist by the Environmental Research Laboratories of the National Oceanic and Atmospheric Administration, Boulder, CO. Since joining the Boulder Laboratories of the U.S. Department of Commerce in 1960, his research has been concerned with microwave absorption in the atmosphere, microwave and infrared radiative transfer, ground- and satellite-based remote sensing by passive radiometry, and in the application of mathematical inversion techniques to problems in remote sensing.

Dr. Westwater is a member of the American Meteorological Society, the Mathematical Association of America, the Society for Industrial and Applied Mathematics, the Optical Society of America, and the American Association for Advancement of Science.